

Relations between PET-derived measures of thalamic glucose metabolism and EEG alpha power

CHRISTINE L. LARSON,^a RICHARD J. DAVIDSON,^{a,b} HEATHER C. ABERCROMBIE,^a
ROBERT T. WARD,^a STACEY M. SCHAEFER,^a DAREN C. JACKSON,^a
JAMES E. HOLDEN,^c AND SCOTT B. PERLMAN^d

^aDepartment of Psychology, University of Wisconsin, Madison, USA

^bDepartment of Psychiatry, University of Wisconsin, Madison, USA

^cDepartment of Medical Physics, University of Wisconsin, Madison, USA

^dDepartment of Radiology, University of Wisconsin, Madison, USA

Abstract

Electroencephalogram (EEG) alpha power has been demonstrated to be inversely related to mental activity and has subsequently been used as an indirect measure of brain activation. The thalamus has been proposed as an important site for modulation of rhythmic alpha activity. Studies in animals have suggested that cortical alpha rhythms are correlated with alpha rhythms in the thalamus. However, little empirical evidence exists for this relation in humans. In the current study, resting EEG and a fluorodeoxyglucose positron emission tomography scan were measured during the same experimental session. Over a 30-min period, average EEG alpha power across 28 electrodes from 27 participants was robustly inversely correlated with glucose metabolic activity in the thalamus. These data provide the first evidence for a relation between alpha EEG power and thalamic activity in humans.

Descriptors: Electroencephalography, Positron emission tomography, Alpha, Thalamus

Alpha electroencephalogram (EEG) power is a commonly used measure of regional brain activity. It reflects an awake but resting state and is putatively inversely related to neural activity (Shagass, 1972). The thalamus has been hypothesized to be an important source of afferent projections that modulate cortical alpha rhythms (Andersen & Andersson, 1968; Buzsaki, 1991; Jasper, 1949). A substantial body of data from animal studies supports this hypothesis. Performing some of the earliest work in this area, Morison demonstrated that thalamic oscillations in the 8–12-Hz range were present in both corticate (Morison, Finley, & Lothrop, 1943) and decorticate (Morison & Bassett, 1945) cats. Therefore, thalamic rhythmic activity was shown to be present independent of cortical influences.

Subsequently, numerous workers have found substantial relations between rhythmic activity of the thalamus and the neocortex in animals (Andersen, Andersson, & Lømo, 1967a, 1967b; Lopes

da Silva, van Lierop, Schrijer, & Storm van Leeuwen, 1973a). Work by Andersen et al. (1967a, 1967b) first elucidated these relations in studies with anesthetized animals. They demonstrated that in anesthetized cats, spontaneous barbiturate spindles in cortex were highly correlated with thalamic spindle activity and that the thalamus was likely the source for these rhythms. Andersen and Andersson (1968) postulated the existence of not just one but multiple thalamic “pacemakers.” They suggested that any thalamic nucleus was capable of exhibiting rhythmic oscillations and that these oscillations would be synchronized in the thalamus by a “distributor” with wide-ranging intranuclear connections. This rhythm would then be imposed on the cortex via thalamocortical cells.

Lopes da Silva et al. (1973a) found that alpha rhythms in unanesthetized animals differed from the barbiturate spindles produced by anesthetized animals. Therefore, they set out to demonstrate the relations between cortical and thalamic activity in animals that were awake (Lopes da Silva, van Lierop, Schrijer, & Storm van Leeuwen, 1973b). Electrical recordings were made from regions of the thalamus and cortex, especially in the occipital lobe, in six awake, unanesthetized dogs. They examined the coherence between alpha rhythms in the thalamus and cortex. For each of the six dogs, corticocortical coherences were substantially higher than thalamocortical coherences. However, for five of the six dogs, significant thalamocortical coherences were present. They stated that, “as a general rule it may be said that when alpha rhythms were recorded at the cortex they were simultaneously encountered in the thalamus” (p. 631). Thalamocortical coherences were highest for the lateral geniculate nucleus (LGN) of the thalamus. In addition, the coherences between a single electrode in the thalamus

Support for this research was provided by NIMH grants MH40747 and MH43454, NIMH Center grant P50-MH52354 to the Wisconsin Center for Affective Science, a grant from the John D. and Catherine T. MacArthur Foundation, and by an NIMH Research Scientist Award to R. J. Davidson (K05-MH00875).

We thank Andrea Straus, Joni Hanson, Robert Pyzelski, Dan McGary, Heidi Neudeck, and Nicole Kallimanis for their sizable contributions in collecting these data. A subset of these data was presented at the 36th Annual Meeting of the Society for Psychophysiological Research in Vancouver, October 17–20, 1996.

Address reprint requests to: Richard J. Davidson, University of Wisconsin, Department of Psychology, 1202 West Johnson Street, Madison, WI 53706, USA. E-mail: davidson@macc.wisc.edu.

and various cortical electrodes were sometimes different, even when the cortical electrodes were as little as 1 mm apart. Lopes da Silva et al. interpreted this observation as general support for Andersen and Andersson's (1968) hypothesis of multiple, as opposed to a single, thalamic "pacemakers."

Due to the high corticocortical coherences found in this study, Lopes da Silva, Vos, and Van Rotterdam (1980) performed another study in the same dogs to determine the extent to which these large intracortical coherences were influenced by the thalamus. To examine thalamic contributions to corticocortical coherences, partial coherences were computed. The signal from the thalamus was partialled from each of the two cortical electrodes in a pair, and coherence analyses were performed on these residuals. They found that for most pairs of cortical electrodes the intracortical coherence decreased significantly after partialling out the thalamic contributions and that this effect was much larger for electrodes in the pulvinar nucleus than in the LGN. Therefore, the thalamic influence on corticocortical coherences is substantial, although the extent of this influence is greater for the pulvinar nucleus than for the LGN. Also, despite the large decrease in intracortical coherence following this regression procedure, in most cases significant corticocortical coherence was still present. The studies by the Lopes da Silva group demonstrate the presence of thalamocortical coherences, that the thalamus contributes significantly to corticocortical coherences, and that in general these intracortical coherences remain even after removing the thalamic contributions. This finding suggests that both thalamic and nonthalamic sources contribute to modulation of alpha rhythms.

More recently, Steriade, Deschenes, Domich, and Mulle (1985) continued to examine the role of the thalamus in cortical rhythmic activity. In contrast to Andersen and Andersson's model (1968), which suggests that any of the thalamic nuclei is capable of exhibiting rhythmic oscillations and imposing this rhythm on other nuclei, Steriade et al. proposed that the nucleus reticularis in the thalamus is the true "pacemaker." Selective damage to this nucleus abolished rhythmic activity of the thalamus and cortex in rats (Buzsaki, Bickford, Ponomareff, Thal, Mandel, & Gage, 1988) and cats (Steriade et al., 1985). In addition, very few connections have been observed among most thalamic nuclei (Jones, 1985). Only the nucleus reticularis projects to virtually all other thalamic nuclei (Scheibel & Scheibel, 1966). Therefore, it was suggested that the nucleus reticularis serves as the pacemaker and imposes its rhythmic oscillation on other thalamic nuclei and thalamocortical cells.

Steriade and colleagues further demonstrated that different frequency oscillations in the nucleus reticularis are associated with different degrees of cellular membrane polarization. They demonstrated that in the nucleus reticularis of the thalamus, spindle-like oscillations between 7 and 14 Hz were associated with resting membrane potentials (approximately -60 mV) (Steriade & Deschenes, 1984; Steriade, Dossi, & Nunez, 1991). Membrane hyperpolarization was associated with 1–4-Hz rhythms (Steriade, Dossi, & Nunez, 1991) and depolarization with 40-Hz oscillations (Steriade, Dossi, Pare, & Oakson, 1991). These different rhythmic patterns are thought to be implemented in the cortex via thalamic relay nuclei. Therefore, because 7–14-Hz rhythms of the nucleus reticularis are associated with resting membrane potentials, we would expect that the presence of cortical alpha rhythms would be associated with an absence of activation of this nucleus in the thalamus. Cortical alpha activity and nucleus reticularis activation should be inversely correlated.

Although these animal studies have been of great importance for outlining the cellular neurophysiology of the relations between

thalamic and cortical rhythmic activity, these issues have yet to be investigated in humans. Although Lopes da Silva et al. (1973a) suggested that the rhythmic activity of the dogs in their study was similar to that of humans in terms of frequency band, topography, and the conditions that elicited alpha, our understanding of the neurophysiology of alpha rhythms will be greatly enhanced by human data. With the advent of neuroimaging procedures, examination of thalamocortical relations in intact human subjects is now possible.

In the current study, we examined the relation between EEG measures of cortical alpha power and thalamic glucose metabolic rate measured with positron emission tomography (PET). When examining the relations between EEG activity and glucose metabolism, one important methodological consideration is the degree to which the two measures reflect the same underlying process. Neuronal activity (e.g., synaptic transmission, excitation, and inhibition) requires energy, and glucose metabolism is almost exclusively the sole source of this energy (Roland, 1993). Roland cited many sources of evidence in support of the coupling of neuronal activity and glucose metabolism. In one such study, Astrup, Sorensen and Sorensen (1981) examined resting glucose metabolism in a dog and systematically blocked aspects of neuronal activity that require glucose metabolism for energy. They first anesthetized dogs to the point at which no electrical activity was detected from the dogs' brains. This level of anesthesia reduced the glucose consumption to 70% of the resting metabolic rate before anesthetizing the dog. Next, the researchers blocked two other energy-consuming neuronal processes. Using lidocaine and ouabain, the Na^+ channels and the Na^+/K^+ pump were blocked. This procedure reduced the rate of glucose metabolism to 35% of what it had been originally during the resting condition. Additional blocks on other neuronal processes were not carried out because they could have been fatal to the animal. However, these data clearly indicate that neural activity is largely fueled by the metabolism of glucose.

A further consideration regarding the relations between EEG and the measurement of glucose metabolism concerns detecting differences between neuronal excitation and inhibition using PET imaging. Two important issues must be kept in mind when considering this question. First, *in vivo* methods of glucose metabolism, including PET, all sample from relatively large tissue sections. Within any such tissue sample, there is a large number of cells, all of which can potentially have multiple inhibitory and excitatory synapses converging upon them. What is measured by PET estimates of glucose metabolism is the summation of these multiple excitatory and inhibitory effects in a given region of tissue. Moreover, glucose metabolism is required for both excitatory and inhibitory events to occur. The downstream effects of excitatory and inhibitory processes will obviously be different but they cannot be differentiated at the site of initiation. This limitation is inherent to all metabolic or hemodynamic imaging procedures and requires correlational techniques to determine if activation in one brain region is systematically associated with inhibition elsewhere. The methods required for such studies are still under development but represent promising new directions in discriminating excitatory from inhibitory effects.

In the current study, PET and EEG were recorded at the same session to assess the association between alpha power and glucose metabolism in the thalamus. Because the temporal resolution of PET is vastly inferior to that of EEG (about 30 min for the approach used in the current work), this study could not assess thalamic activity in relation to the phasic aspects of alpha rhythms. In addition, the spatial resolution of PET is not sufficient to discrim-

inate separate nuclei of the thalamus. Therefore, across a group of 27 participants, we examined the relationship between metabolic activity of the entire thalamus and a simultaneously collected measure of alpha power aggregated over a 30-min period. These data were collected as part of a study comparing regional brain activation in depressed and nondepressed individuals. We did not expect relations between alpha power and metabolic rate in the thalamus to differ between depressed and nondepressed participants. In line with the findings of Steriade and Deschenes (1984), we expected metabolic activity in the thalamus to be inversely correlated with alpha power. In other words, greater metabolic rate in the thalamus was expected to be correlated with greater alpha suppression.

Method

Participants

The current data were collected as part of a study comparing resting regional brain metabolic and electrocortical activity in depressed and nondepressed participants. Participants were recruited via advertisements in local newspapers and on local TV and radio stations. Respondents were screened by telephone, and potential participants with medical conditions contraindicating a PET scan were rejected. Those individuals likely to meet study criteria were invited in for a diagnostic interview. Participants were screened for psychopathology using the Structured Clinical Interview for the *Diagnostic and statistical manual of mental disorders* (3rd ed., rev. ed.), Patient Edition (SCID-P; Spitzer et al., 1990). All depressed participants were required to meet *DSM-IV* criteria (American Psychiatric Association, 1994) for major depression. Control participants had no past history of any Axis I disorders and no family history of Axis I disorders. All participants were required to be off any form of antidepressant medication for at least 4 weeks before testing. Participants were right handed as assessed by the Chapman Handedness Inventory (Chapman & Chapman, 1987).

Thirty individuals participated in the study; however, three were not included in data analysis because of technical problems with the PET data. Therefore, a total of 27 participants (14 women) were used in analyses for this study, 19 depressed (10 women) and 8 nondepressed controls (4 women). The two groups did not differ in age (depressed, $M = 36.00$ years, range = 20–54 years; controls, $M = 37.63$ years, range = 22–57 years), $t(25) = .36$, $p > .25$.

Procedures

Participants completed a full day of testing including EEG assessment and measurement of resting regional cerebral glucose metabolic rate (rCMRglu) using [^{18}F]-2-fluoro-2-deoxy-D-glucose positron emission tomography (FDG-PET). The EEG data were collected at the same time as the PET procedures, which took place midway through the test day, just following an event-related potential (ERP) assessment. The sessions were run at the University of Wisconsin PET Imaging Center. Participants fasted for 5 h before arrival at the PET Center. Upon arrival, participants were seated in a chair in the PET scanning room, and an overview of the PET and EEG procedures was provided. For 16 participants (10 depressed, 6 control) ERPs were recorded during the testing segment just before, so participants arrived already fitted with the EEG and electrooculogram (EOG) recording electrodes. The electrode cap and EOG electrodes were rechecked for placement and impedances. For the 11 participants who did not arrive with the electrodes already in place, the EEG and EOG electrodes were placed at this time.

After the electrodes were checked and connected, both of the participant's hands were placed in hand-warming boxes used to increase blood flow through the hands and facilitate blood drawing for the PET procedure. The left hand was placed into a heated hand warmer to maintain a skin surface temperature of 42°C, which allowed for rapid sequential sampling of "arterialized" blood. The right hand was also heated to equate thermal stimulation on both sides of the body. Once the participant's hands had been sufficiently warmed, two intravenous lines (22-gauge intravenous catheters) were placed by an experienced technologist. One line was placed in the antecubital fossa of the right arm, and the other on the posterior aspect of the left hand.

Participants were instructed that after the FDG was injected the uptake period would last 30 min, during which the room would be kept as quiet as possible. A 1–2-ml blood sample was drawn to obtain an initial plasma glucose level. Just before injection of the radiotracer, the participants were informed that EEG recording was to start and whether to hold their eyes open or closed. Five milluries of FDG were then administered by bolus injection into the intravenous line in the right arm, beginning a 30-min period during which the isotope was taken up by the body. Throughout the 30 min, a technologist seated to the left of the participant drew blood samples from the left hand for measurement of blood glucose levels and the time course of the radiotracer in plasma. A laboratory assistant who recorded the exact time of each blood draw was also seated to the participant's left.

Sequential 1–2-ml blood samples were collected throughout the uptake period as follows: every 15 s for 2 min; every 30 s for the next 2 min; every minute for the next 4 min; every 2 min for the next 10 min; and every 3 min for the next 12 min. These samples were used to determine the time course of the concentration of tracer in plasma. In addition, two samples were obtained to measure plasma glucose levels at approximately 15 and 30 min postinjection.

EEG collection began at the time of injection. Ten contiguous 3-min trials of EEG data were recorded to cover the entire 30 min. Each trial alternated between eyes open and eyes closed conditions, with the starting condition counterbalanced across participants.¹ The experimenter verbally informed the participant of the trial condition before beginning each 3-min trial. At the end of 30 min, the intravenous lines and EEG cap and EOG electrodes were removed. The participant was placed in the PET scanner bed to acquire a 30-min emission scan.² Following the scan, a lunch was provided and the participants were escorted from the PET Center to the site of the next test assessment.

EEG Recording and Quantification

EEG was recorded using a modified Lycra electrode cap (Electro-Cap), positioned on the participant's head using known anatomical landmarks (Blom & Anneveldt, 1982). EEG was recorded at 28 scalp sites (FP1/2, F3/4, F7/8, FT3/4, FT7/8, C3/4, T3/4, T5/6,

¹An alternating sequence of eyes open and eyes closed trials was used because previous work in our laboratory has demonstrated that an aggregate of both eyes open and eyes closed data yields the most reliable estimates of spectral power asymmetry (see Tomarken, Davidson, Wheeler & Kinney, 1992).

²The PET scan procedure can be somewhat anxiety provoking (e.g., needle sticks, blood draws, injection of the radiotracer). However, the EEG data and PET metabolic data putatively reflect brain activity from the same period (most of the PET radiotracer is absorbed during the 30-min uptake period). Therefore, the two measures should not be affected differentially by any anxiety elicited by the procedures.

CP3/4, CP5/6, P3/4, PO3/4, FPZ, FZ, CZ, and PZ) referenced to the left ear (A1). The right ear (A2) was also recorded for rederivation of a linked ears reference off-line. To visually score data for eye movement artifact, two channels of EOG were recorded: horizontal (HEOG) from the external canthi of each eye and vertical (VEOG) from the supra- to suborbit of one eye. All EEG electrode impedances were under 5,000 Ω , and the impedances of homologous sites were within 2,000 Ω . EOG electrode impedances were under 20,000 Ω . The EEG and EOG were amplified with a Grass Model 12 Neurodata System using Model 12C preamplifiers, with a bandpass of 1–300 Hz and a 60-Hz notch filter. The signal was also filtered with MF6 digital anti-aliasing low-pass filters set at 100 Hz, with a 36 dB/octave roll-off. The signals were digitized on-line at 250 Hz by a 486 DX2-33 MHz PC and an Analogic MS-DAS-12 A/D board.

The EEG was visually scored and edited to remove artifact due to eyeblinks, gross muscle activity, and movement. When an artifact occurred in a given channel, data from all channels were removed. Artifact-free chunks of data were extracted through a Hamming window, which reduces spurious spectral power estimates at the beginning and end of each chunk. A fast Hartley transform (FHT; Bracewell, 1984) was applied to all extracted artifact-free epochs of data that were 1.024 s in duration, with epochs overlapping 50%. The mean number of seconds of artifact-free data was 994.66 ($SD = 216.85$). Data were referenced off-line to the average reference. Power density ($\mu V^2/Hz$) was then computed for the alpha band (8–13 Hz). Power density was computed by summing power values across each 1-Hz bin within the band and dividing by the number of bins. Trials with less than 30 s of artifact-free EEG were dropped from future computations. Mean alpha power was computed for the five trials in each condition (eyes open and eyes closed). All power density values were log transformed to normalize the distribution of the data. To compare whole-head alpha power with metabolic rate, mean alpha power across all 28 electrodes was computed for the eyes open and eyes closed conditions. One (depressed) participant did not have a sufficient amount of artifact-free eyes closed data, and the data were dropped from the analyses. Therefore, eyes open comparisons were done with the full sample of 27 participants and eyes closed comparisons with 26 participants (18 depressed, 8 control). Mean whole-head alpha power across the eyes open and eyes closed conditions was also derived.

PET Data Collection and Reduction

^{18}F fluoride was produced by a CTI RDS Cyclotron (Knoxville, TN) in the Department of Medical Physics. FDG was synthesized using the modified method of Hamacher and Coenen (1986).

Scans were performed with a GE Advance PET camera (Waukesha, WI; in-plane resolution of approximately 4 mm and axial resolution of approximately 5 mm, full width half maximum). A laser positioning device was used to position the participant's head in the scanner. The image planes were positioned parallel to the orbitomeatal line. Thirty-five axial slices covering the entire brain were acquired during a 30-min emission scan. All images were reconstructed to 128×128 pixels, yielding in-plane pixel dimensions of $2.34 \text{ mm} \times 2.34 \text{ mm}$. Calculated attenuation correction was applied to the data. Planes containing tissue inferior to the temporal lobes were excluded, thus yielding 24 planes superior to the inferior temporal lobe that were used for subsequent analyses. These 24 planes were reformatted to $128 \times 128 \times 46$. Pixel dimensions were $2 \text{ mm} \times 2 \text{ mm} \times 4 \text{ mm}$.

To determine absolute scaling of metabolic rate, the emission data were quantitated using the following procedures. Aliquots of plasma were obtained from each blood sample and plasma radioactivity concentrations were measured. Radioactivity values were corrected for physical decay back to the time of injection. Previous measurements in our laboratory demonstrated the striking similarity, up to a multiplicative scale, of plasma FDG concentration time courses following the initial distribution of tracer into the plasma and extracellular spaces. The individual plasma time courses measured over the first 30 min were thus combined with previously measured normative data to provide tracer concentration time courses over the duration of the PET image data acquisition. These plasma time courses were combined with plasma glucose levels and image pixel values to estimate the rate of glucose utilization of each image pixel according to the Sokoloff method (Sokoloff et al., 1977).

Using Statistical Parametric Mapping software (SPM 95; MRC Cyclotron Unit, Hammersmith Hospital, London, England; Friston, Dolan, & Frackowiack, 1991), the PET scans were stereotactically normalized using a nonlinear transformation to a standardized coordinate system (Talairach & Tournoux, 1988). A $20 \text{ mm} \times 20 \text{ mm} \times 12 \text{ mm}$ Gaussian filter was applied to the scans to reduce error due to small morphological differences among participants. Following transformation, global differences in CMRglu were removed using the SPM analysis of covariance (ANCOVA) procedure. The ANCOVA was performed separately for the depressed and control groups.

Statistical Analysis

Four t tests were performed to examine group differences. First, two t tests were conducted comparing the depressed and control groups on average eyes open and average eyes closed alpha power from all 28 electrodes. A third between-groups t test was performed to determine whether or not the two groups differed on global CMRglu (average CMRglu from the entire brain volume). The final t test compared the depressed and control groups on rCMRglu from one pixel in the right thalamus (10, -18, 16). This pixel was used throughout the subsequent analyses as a representative of relations between alpha power and metabolism in the thalamus. Use of a single pixel simplified the analysis and is justified by the $20 \text{ mm} \times 20 \text{ mm} \times 12 \text{ mm}$ Gaussian filter applied to the image data, which imposes extremely high degrees of correlation between neighboring pixels. In an unpublished trial performed in our laboratory, correlations between the mean values in a $5 \times 5 \times 3$ pixel volume ($10 \text{ mm} \times 10 \text{ mm} \times 12 \text{ mm}$) and the single pixel at its center ranged from .985 to .998 (Davidson, Ward, Abercrombie, & Schaefer, 1997). Therefore, we determined that using a single pixel for these representative correlations was sufficient. This pixel was chosen as the representative because it was clearly within the Talairach coordinates that include the thalamus (Talairach & Tournoux, 1988).

Three sets of correlations were run, all of which compared a measure of alpha power with metabolic data from every pixel in the PET image across subjects. These correlations were performed using the SPM correlation method, which tests the correlation of a variable (in this case, alpha power) with rCMRglu for every pixel in the normalized brain volume and applies a correction for multiple comparisons. Given that we had no hypotheses for group differences in the relations between alpha power and thalamic activity, all of the correlations were performed using participants from both groups combined. The same PET image data was used for all three sets of correlations. Only the alpha power metric used in the correlations differed. The first set correlated rCMRglu with

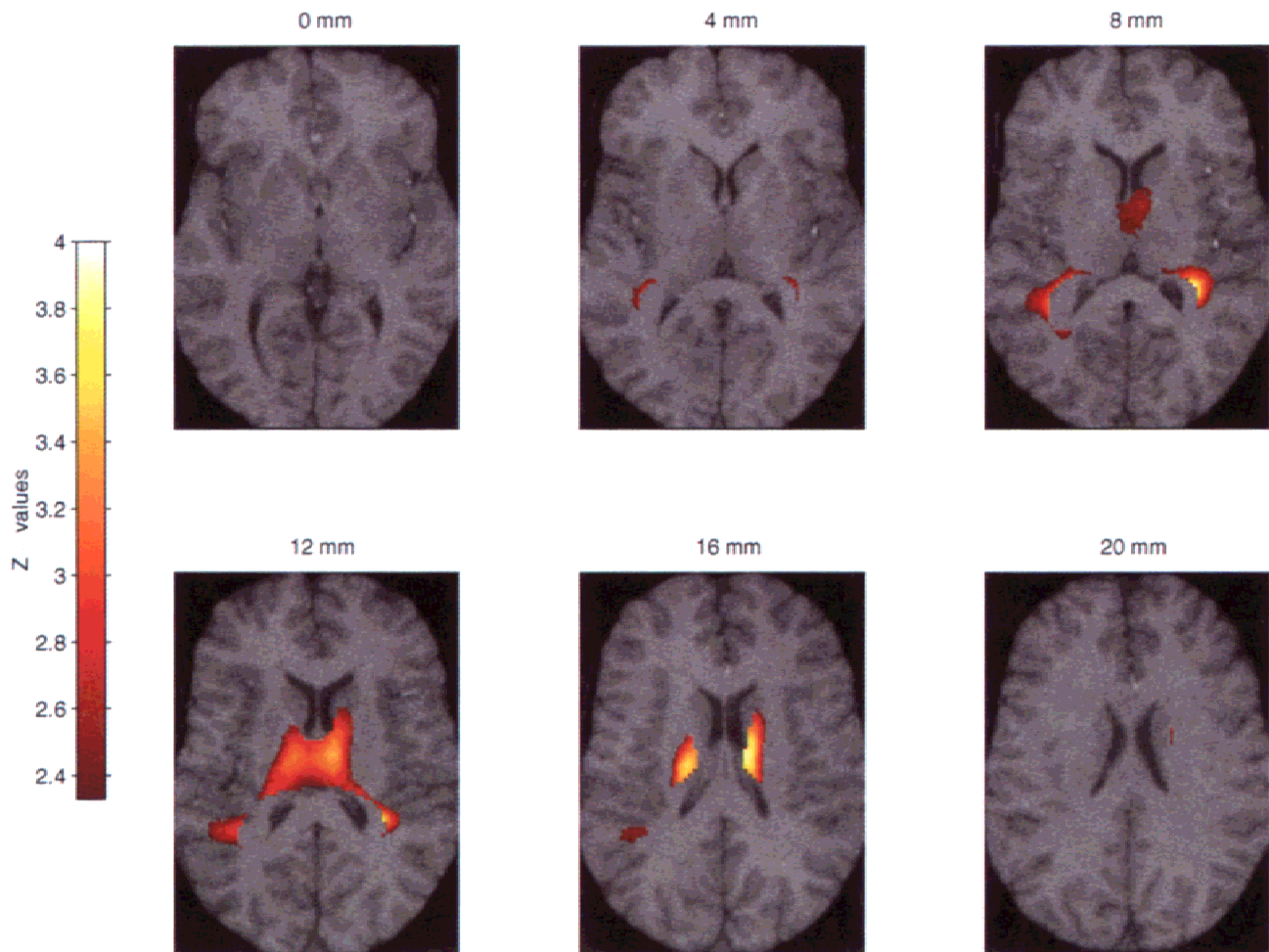


Figure 1. Negative correlations between rCMRglu from the entire brain volume and eyes open average 8–13 Hz alpha power from all 28 electrodes mapped onto axial MRI planes spanning the thalamus. The scale is in z values. The lowest z value displayed is 2.33, which is equivalent to an r threshold of .43.

mean alpha power from all 28 electrodes for the eyes open and eyes closed alpha power separately.³ The second set examined the relationship between rCMRglu and mean whole-head alpha power separately for low (8–10 Hz) and high (10–13 Hz) alpha power. Finally, the third set of correlations tested the relationship between glucose metabolism from the entire brain volume with right and left hemisphere alpha power.

The first set of correlations was designed to compare average alpha power from the whole head with PET glucose metabolic data across subjects. Therefore, two correlations were performed including participants from both groups, one comparing eyes open alpha power across all 28 electrodes and rCMRglu from every pixel in the PET image. A second identical correlation was run for the eyes closed condition.

³Average alpha power from all 28 electrodes was used for these correlations because all electrodes showed similar significant correlations with rCMRglu in the thalamus. Using rCMRglu from the representative pixel in the right thalamus (10, -16, 18) that was used for all analyses reported in this article, the correlations between rCMRglu and eyes open alpha power ranged between $-.50$ and $-.68$ ($ps < .007$) for the 28 leads. The correlations between this pixel and eyes closed alpha power for the 28 leads ranged between $-.45$ and $-.63$ ($ps < .02$).

Factor analytic techniques have shown the alpha band to “split” at 10 Hz (Andresen, 1993; Goncharova & Davidson, 1995). Accordingly, we performed a second set of correlations in which the data were analyzed separately for low (8–10 Hz) and high (10–13 Hz) alpha bands. Two SPM correlations were performed, correlating alpha power PET metabolic rate from each pixel separately for the low and high alpha bands. These correlations were performed with the alpha power data collapsed across the eyes open and eyes closed conditions.

To examine whether or not relations differed between the two hemispheres, SPM correlations were performed correlating rCMRglu from every pixel with 8–13 Hz alpha power for the left hemisphere (FP1, F3, F7, FT3, FT7, C3, T3, T5, CP3, CP5, P3, PO3) and right hemisphere (FP2, F4, F8, FT4, FT8, C4, T4, T6, CP4, CP6, P4, PO4) separately. These correlations were performed using alpha power from the eyes open and eyes closed conditions averaged together.

Results

T Tests on Dependent Measures

T tests comparing the two groups on alpha power revealed that the two groups did not differ on average alpha power for either the

eyes open condition (controls, $M = .21$, $SD = 1.37$; depressed, $M = -.04$, $SD = .96$), $t(25) = -.53$, $p > .25$, or the eyes closed conditions (controls, $M = .78$, $SD = 1.26$; depressed, $M = .51$, $SD = .97$), $t(24) = -.59$, $p > .25$. Global $rCMRglu$ did not differ between depressed and control participants (controls, $M = 4.93$, $SD = .35$; depressed, $M = 4.66$, $SD = 1.02$), $t(25) = .47$, $p > .25$. The two groups also did not differ on $rCMRglu$ in the representative pixel chosen from the right thalamus (10, -18, 16) (controls, $M = 4.85$, $SD = .58$; depressed, $M = 5.07$, $SD = .31$), $t(25) = .20$, $p > .25$.

Whole-Head Alpha Power for the 8–13-Hz Band

For the correlations comparing whole-head alpha power from the 8–13-Hz band, robust and consistent correlations with global alpha power were found in a region including the thalamus. These correlations were inverse (range in r s = $-.45$ to $-.59$, p s < $.001$), indicating that greater thalamic metabolism is correlated with decreased alpha power. Maps of the negative correlations are presented separately for the eyes open and eyes closed alpha power data (see Figures 1 and 2). These maps depict correlations that exceeded a threshold of $r = -.43$. The maps cover brain tissue between the AC–PC line (0 mm) and 20 mm superior to the AC–PC

line. These six planes span the Talairach coordinate planes that include the thalamus.

There were no positive correlations that exceeded threshold for either the eyes open or eyes closed condition in any of the six planes displayed in Figures 1 and 2 (spanning brain tissue between 0 mm, AC–PC line and 20 mm superior to the AC–PC line), including the region of the thalamus.

Scatterplots of a representative negative correlation between $rCMRglu$ in one pixel in the right thalamus (10, -18, 16) and alpha power are presented separately for eyes open and closed EEG data (see Figure 3; for eyes open, $r = -.59$, $p < .001$; for eyes closed, $r = -.52$, $p < .001$).

Low Versus High Alpha

The correlations between thalamic $rCMRglu$ and alpha power did not differ for the low (8–10 Hz) and high (10–13 Hz) alpha bands. The correlations that exceeded threshold ranged from $-.46$ to $-.59$ (p s < $.001$) for both subalpha bands. The correlation between $rCMRglu$ in the same pixel in the right thalamus (10, -18, 16) and low and high alpha power were nearly identical. For the low alpha band, $r = -.57$ ($p < .001$), and for the high alpha band, $r = -.56$ ($p < .001$).

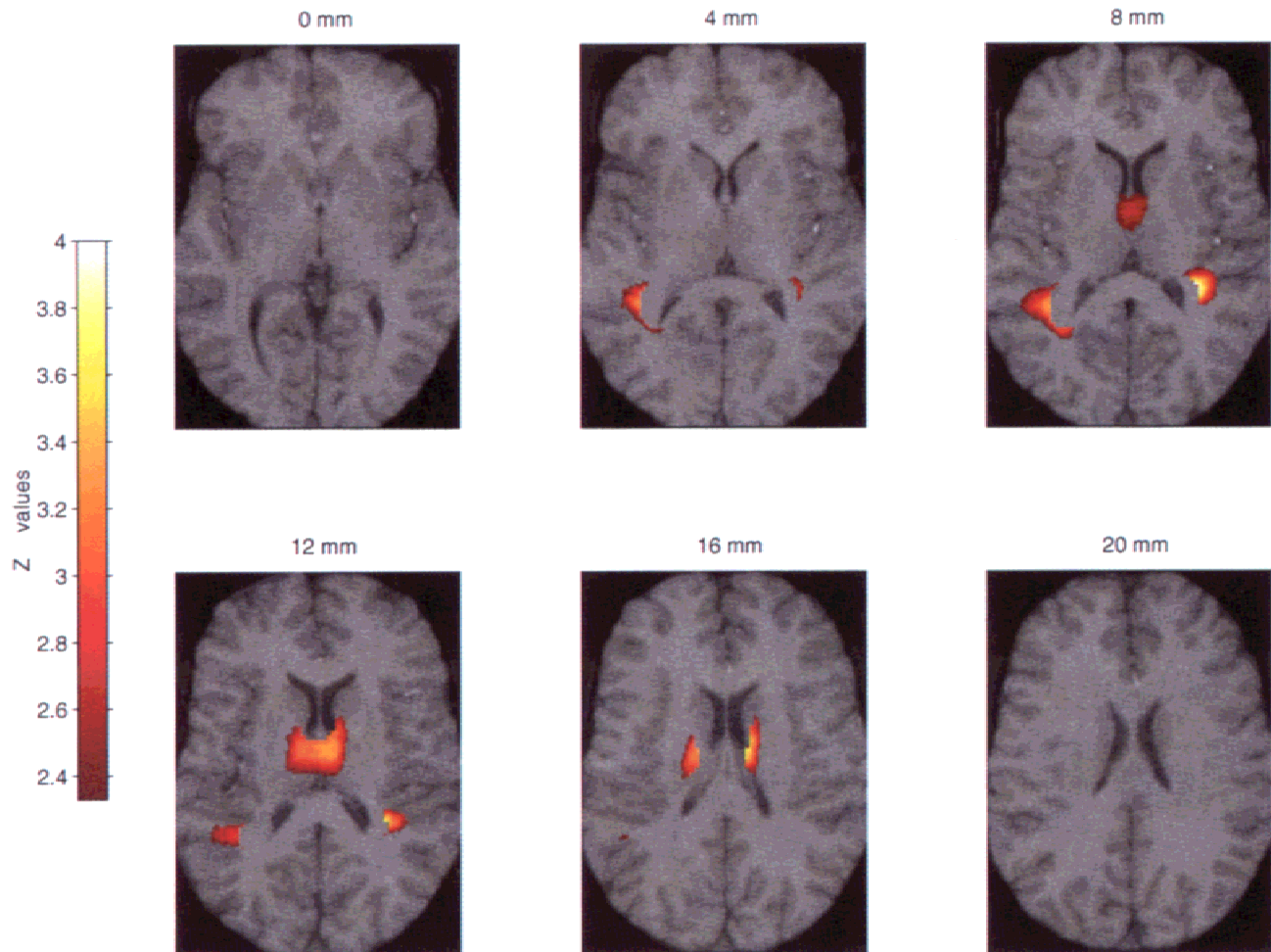


Figure 2. Negative correlations between $rCMRglu$ from the entire brain volume and eyes closed average 8–13 Hz alpha power from all 28 electrodes mapped onto axial MRI planes spanning the thalamus. The scale is in z values. The lowest z value displayed is 2.33, which is equivalent to an r threshold of $.43$.

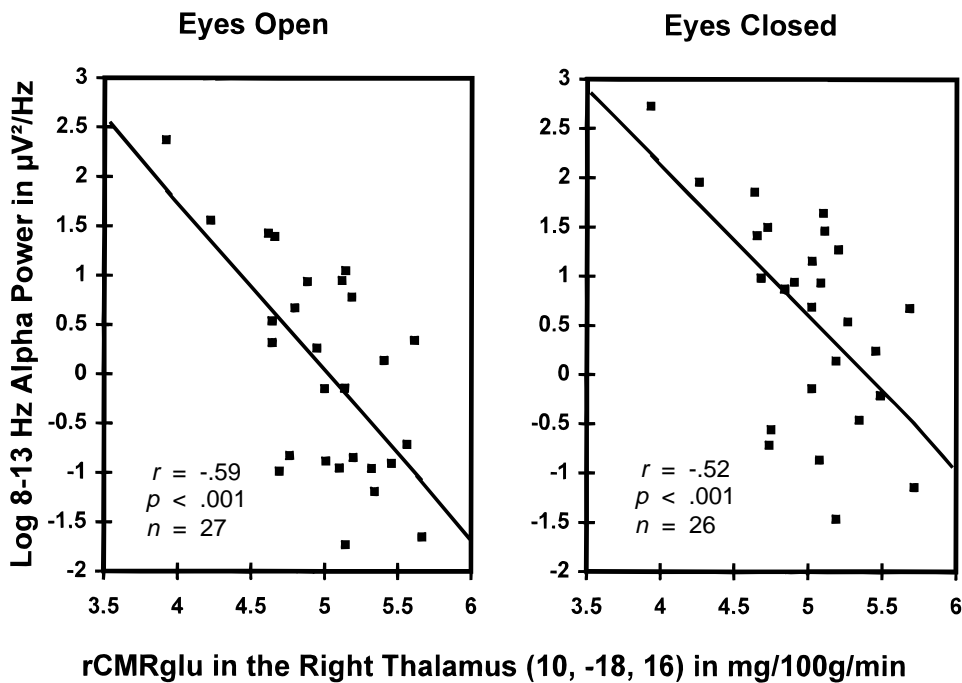


Figure 3. Scatter plots of the correlations between rCMRglu from one coordinate in the right thalamus (10, -18, 16) and eyes open and eyes closed average 8–13 Hz alpha power from all 28 electrodes.

Left Versus Right Hemisphere

Correlations between alpha power and rCMRglu in the region of the thalamus were also similar for EEG alpha power from the left and right hemispheres. For right hemisphere, alpha power and metabolic rate in the thalamus, r s ranged from $-.46$ to $-.58$ (p s $< .001$). For the left hemisphere, r s ranged from $-.46$ to $-.60$ (p s $< .001$). The correlation for the representative pixel in the right thalamus (10, -18, 16) was $-.56$ ($p < .001$) for right hemisphere alpha power and $-.58$ ($p < .001$) for left hemisphere alpha power.

Discussion

These data indicate that over a 30-min time period an aggregate measure of power in the alpha band is inversely correlated with glucose metabolic rate in the thalamus from the same 30-min period. Although alpha rhythms are generally more predominant during eye closure, no differences were observed between the correlations for the eyes open and eyes closed conditions. These correlations were also the same for both the low and high alpha bands and for alpha power from both hemispheres. Furthermore, these robust negative correlations were fairly specific to the thalamus. Only one other region, the most medial portion of the superior temporal gyrus, showed negative correlations that exceeded the set threshold. The meaning of these superior temporal gyrus correlations is unclear. Finally, no positive correlations were found that exceeded threshold anywhere in the brain volume. Thus, across time, greater thalamic metabolism is associated with alpha suppression rather than with alpha activity.

These data are congruent with the findings of Steriade and colleagues, who reported that in the nucleus reticularis of the thalamus oscillations in the alpha band were associated with resting membrane potentials (Steriade & Deschenes, 1984; Steriade, Dossi, & Nunez, 1991; Steriade, Dossi, Pare, et al., 1991). Although the resolution of PET imaging is not capable of distinguishing individual nuclei within the thalamus, these data are broadly consistent

in that cortical alpha power is correlated with decreased metabolism in the thalamus. According to Steriade's findings, we would expect that this idling rhythm of the thalamus originates in the nucleus reticularis, is then impressed on other thalamic nuclei, and is relayed to the cortex via thalamocortical relay cells. Because regional metabolic rate putatively reflects regional neuronal activity, our finding of an association between decreased thalamic metabolic rate and increases in alpha power is consistent with Steriade's finding of resting potentials in the thalamus associated with rhythmic activity in the alpha band. These data provide an initial demonstration of how the combination of PET and EEG techniques can be used to extend findings from animal studies to humans.

Although Buzsaki (1991) and others have attributed neocortical activity to thalamocortical circuits exclusively, other workers, notably Nunez (1995), have proposed that the neocortex determines the resonant oscillatory activity of the brain. Whereas Nunez does include the thalamus in the neural circuitry underlying these rhythmic oscillations, based on work by Steriade, Oakson, and Diallo (1976), Nunez proposed that the thalamus adjusts its oscillatory frequencies to be synchronous with the neocortical resonant frequency. This frequency plasticity was demonstrated by stimulating the motor cortex electrically with a 10-Hz pulse delivered every 2 s. After 28 passes, the thalamic nuclei began to produce spontaneous bursts of rhythmic activity near this 10-Hz driving frequency (Steriade et al., 1976). Furthermore, thalamic oscillations that are coincident with neocortical rhythms will produce a larger cortical response than a thalamic rhythm that is unrelated to the neocortical resonant frequency. Nunez suggested that the combination of the larger neocortical response and the frequency plasticity of the thalamus causes the thalamic rhythms to become coincident with the neocortical rhythms. Again, because the data we have presented are correlational, we cannot make inferences about the causal status of a thalamic pacemaker in regulating the frequency of cortical rhythmicity. Future work in this area will need to consider both the thalamic multiple pacemaker hypothesis and Nunez's neocortical modulation hypothesis.

Several limitations of the present findings must be underscored. First, given that these data are averaged over 30 min, the data provide only a coarse examination of the temporal and phasic aspects of the relations between alpha power and thalamic activity. Second, because these data are correlational, they cannot be used to address whether or not the thalamus is the source of cortical alpha rhythms. Third, although correlations were performed separately for the eyes open and eyes closed alpha power, because of the nature of FDG-PET the metabolic data were always aggregated across both conditions. Finally, the use of the SPM correlation method necessitates including all pixels from the entire brain volume in the correlation and using atlas-based coordinates for localizing the thalamus in stereotactically transformed brain images. A more precise method would be to use structural magnetic resonance imaging (MRI) data from each participant, coregister the MRI to the participant's PET data, and identify the thalamus uniquely for each participant. Metabolic rate from the thalamus could then

be extracted from each participant's PET scan and correlated with alpha power. This method would also eliminate the need for the application of a spatial filter to smooth the data, which would increase the spatial precision with which glucose metabolism in the thalamus could be assessed. Despite the advantages of this method, the current spatial resolution of PET would still not allow for the examination of individual thalamic nuclei, with the possible exception of the largest nuclei, such as the pulvinar.

Whereas previous invasive neurophysiological studies have shown alpha rhythms to be regulated by thalamic activity in other species, this study is the first demonstration of this relation in humans. The combination of neuroimaging and EEG data has potential for enabling us to better understand the neurophysiology of alpha and other rhythmic activity of the brain. In addition, this combination may facilitate our understanding of the role of subcortical structures in phenomena previously studied only with scalp-recorded EEG.

REFERENCES

- American Psychiatric Association. (1994). *Diagnostic and statistical manual of mental disorders* (4th ed.). Washington, DC: Author.
- Andersen, P., & Andersson, S. A. (1968). *Physiological basis of the alpha rhythm*. New York: Century-Crofts.
- Andersen, P., Andersson, S. A., & Lømo, T. (1967a). Some factors involved in the thalamic control of spontaneous barbiturate spindles. *Journal of Physiology*, *192*, 257–281.
- Andersen, P., Andersson, S. A., & Lømo, T. (1967b). Nature of thalamo-cortical relations during spontaneous barbiturate spindle activity. *Journal of Physiology*, *192*, 283–307.
- Andresen, B. (1993). Multivariate statistical methods and their capability to demarcate psychophysiological and neurophysiological sound frequency components of human scalp EEG. In S. Zschocke & E.-J. Speckmann (Eds.), *Basic mechanisms of the EEG* (pp. 317–352). Boston: Birkhäuser.
- Astrup, J., Sorensen, P. M., & Sorensen, H. R. (1981). Inhibition of cerebral oxygen and glucose consumption in the dog by hypothermia, pentobarbital, and lidocaine. *Anesthesiology*, *55*, 263–268.
- Blom, J. L., & Anneveldt, M. (1982). An electrode cap tested. *Electroencephalography and Clinical Neurophysiology*, *54*, 591–594.
- Bracewell, R. N. (1984). The fast hartley transform. *Proceedings of the Institute for Electrical and Electronics Engineers*, *72*, 1010–1018.
- Buzsaki, G. (1991). The thalamic clock: Emergent network properties. *Neuroscience*, *41*, 351–364.
- Buzsaki, G., Bickford, R. G., Ponomareff, G., Thal, L. J., Mandel, R., & Gage, F. H. (1988). Nucleus basalis and thalamic control of neocortical activity in the freely moving rat. *Journal of Neuroscience*, *8*, 4007–4026.
- Chapman, L. J., & Chapman, J. P. (1987). The measurement of handedness. *Brain and Cognition*, *6*, 175–183.
- Davidson, R. J., Ward, R. T., Abercrombie, H. C., & Schaefer, S. S. (1997). [Correlations between rCMRglu from single pixels and cubic voxels]. Unpublished raw data.
- Friston, K. J., Dolan, R. J., & Frackowiack, R. S. J. (1991). *Statistical parametric mapping*. London: MRC Cyclotron Unit, Hammersmith Hospital.
- Goncharova, I. I., & Davidson, R. J. (1995). The factor structure of EEG: Differential validity of low and high alpha asymmetry in predicting affective style [Abstract]. *Psychophysiology*, *32*, S35.
- Hamacher, K., & Coenen, H. H. (1986). Efficient stereospecific synthesis of no-carrier-added 2-[¹⁸F]-fluoro-2-deoxy-glucose using aminopolyether supported nucleophilic substitution. *Journal of Nuclear Medicine*, *27*, 235–238.
- Jasper, H. H. (1949). Diffuse projection systems: The integrative action of the thalamic reticular system. *Electroencephalography and Clinical Neurophysiology*, *1*, 405–420.
- Jones, E. G. (1985). *The thalamus*. New York: Plenum.
- Lopes da Silva, F. H., van Lierop, T. H. M. T., Schrijer, C. F., & Storm van Leeuwen, W. (1973a). Essential differences between alpha rhythms and barbiturate spindles: Spectra and thalamo-cortical coherences. *Electroencephalography and Clinical Neurophysiology*, *35*, 641–645.
- Lopes da Silva, F. H., van Lierop, T. H. M. T., Schrijer, C. F., & Storm van Leeuwen, W. (1973b). Organization of thalamic and cortical alpha rhythms: Spectra and coherences. *Electroencephalography and Clinical Neurophysiology*, *35*, 627–639.
- Lopes da Silva, F. H., Vos, J. E., & Van Rotterdam, A. (1980). Relative contributions of intracortical and thalamo-cortical processes in the generation of alpha rhythms, revealed by partial coherence analysis. *Electroencephalography and Clinical Neurophysiology*, *50*, 449–456.
- Morison, R. S., & Bassett, D. L. (1945). Electrical activity of the thalamus and basal ganglia in decorticate cats. *Journal of Neurophysiology*, *8*, 309–314.
- Morison, R. S., Finley, K. H., & Lothrop, G. N. (1943). Spontaneous electrical activity of the thalamus and other forebrain structures. *Journal of Neurophysiology*, *6*, 243–254.
- Nunez, P. L. (1995). *Neocortical dynamics and human EEG rhythms*. New York: Oxford.
- Roland, P. E. (1993). *Brain activation*. New York: Wiley-Liss.
- Scheibel, M. E., & Scheibel, A. B. (1966). The organization of the nucleus reticularis thalami: A Golgi study. *Brain Research*, *1*, 43–62.
- Shagass, C. (1972). Electrical activity of the brain. In N. S. Greenfield & R. A. Sternbach (Eds.), *Handbook of psychophysiology* (pp. 263–328). New York: Holt, Rinehart, & Winston.
- Sokoloff, L., Reivich, M., Kennedy, C., Des Rosiers, M. H., Patlak, C. S., Pettigrew, K. D., Sakurada, O., & Shinohara, M. (1977). The [¹⁴C]deoxyglucose method for the measurement of local cerebral glucose utilization: Theory, procedure, and normal values in the conscious and anesthetized albino rat. *Journal of Neurochemistry*, *28*, 897–916.
- Spitzer, R. L., Williams, J. B. W., Gibbon, M., & First, M. B. (1990). *Structured clinical interview for DSM-III-R*. Washington, DC: American Psychiatric Press.
- Steriade, M., & Deschenes, M. (1984). The thalamus as a neuronal oscillator. *Brain Research Reviews*, *8*, 1–63.
- Steriade, M., Deschenes, M., Domich, L., & Mulle, C. (1985). Abolition of spindle oscillation in thalamic neurons disconnected from nucleus reticularis thalami. *Journal of Neurophysiology*, *54*, 1473–1497.
- Steriade, M., Dossi, R. C., & Nunez, A. (1991). Network modulation of slow intrinsic oscillation of cat thalamocortical neurons implicated in sleep delta waves: Cortically induced synchronization and brainstem cholinergic suppression. *Journal of Neuroscience*, *11*, 3200–3217.
- Steriade, M., Dossi, R. C., Pare, D., & Oakson, G. (1991). Fast oscillations (20–40 Hz) in thalamocortical systems and their potentiation by mesopontine cholinergic nuclei in the cat. *Proceedings of the National Academy of Sciences, USA*, *88*, 4396–4400.
- Steriade, M., Oakson, G., & Diallo, A. (1976). Cortically elicited spike-wave discharge in thalamic neurons. *Electroencephalography and Clinical Neurophysiology*, *41*, 641–644.
- Talairach, J., & Tournoux, P. (1988). *Co-planar stereotaxic atlas of the human brain*. New York: Thieme.
- Tomarken, A. J., Davidson, R. J., Wheeler, R. W., & Kinney, L. (1992). Psychometric properties of resting anterior EEG asymmetry: Temporal stability and internal consistency. *Psychophysiology*, *29*, 576–592.

(RECEIVED April 2, 1997; ACCEPTED July 1, 1997)